

Fig. 2. Effect of temperature gradient across sample. (C) Corundum, (S) sillimanite (?), (Gl) glass, and (H) higher-temperature side near the heater. Arrow indicates direction to center of cell. (As polished, bright field, $\times 390$.)

considerably cooler than the center. This problem was essentially eliminated by packing so that the final height was about 1.5 mm.

The effects of a less severe gradient across the cell were sometimes seen. In Fig. 2, the part of the sample nearest the heater was hot enough to form corundum, whereas the center of the same run contained only sillimanite (?).^{*} It should be emphasized that the gradient effects were not necessarily detrimental but were very useful and were given considerable weight in interpreting the direction of the reaction at higher temperatures and constant pressure.

(5) Procedure During a Run

All the data were obtained on runs made by first raising the pressure to the desired value and then raising the temperature. The heating rate was about 400°C per minute. At the end of a run, the power to the heater was turned off and the pressure was maintained. The punches and the belt were water-cooled and the sample reached a temperature of 25° to 100°C in about 30 seconds. The pressure was then released and the sample removed.

(6) Starting Materials

The principal starting materials used for the experiments were kyanite from Minas Gerais, Brazil; sillimanite from Idaho and from Dillon, Montana; andalusite from Minas Gerais; and a synthetic $\text{Al}_2\text{O}_3\text{:SiO}_2$ gel. The chemical compositions of these materials are as follows:

Starting material	Wet chemical analysis (wt %)		Remarks
	Al_2O_3	SiO_2	
Kyanite*	62.8	37.4	Blue crystals
Sillimanite	62.8	37.4	White, fibrous, massive
Andalusite	63.4	36.4	Green single crystal
Gel	64.0	36.0	
Theoretical	62.9	37.1	

* Less than 0.2% Fe by X-ray emission analysis.

A few crystals or groups of crystals of kyanite and sillimanite were selected and washed free of external material, if present, and then broken into coarse fragments. From these, clean pieces were selected by handpicking with tweezers under a microscope at $\times 30$. These fragments were then crushed in an alumina mortar and sized by sieving; most of the experiments were with a 50 μ fraction. The homogeneity of the crushed kyanite samples was checked by observation at $\times 500$ in a 1.70 immersion liquid; the kyanite was found to be free of second phases within the resolution of this technique.

The synthetic $\text{Al}_2\text{O}_3\text{:SiO}_2$ gel was made by dissolving the proper amounts of $\text{Al}(\text{NO}_3)_3 \cdot 9\text{H}_2\text{O}$ and ethyl orthosilicate in ethyl alcohol and hydrolyzing to form a gel. The gel was decomposed slowly at 120°C and then heated to 500°C to form an amorphous mixture.

(7) Identification of Phases

The quenched runs were split into two parts along a plane perpendicular to the axis of the cylindrical samples. One half of the sample was crushed and used for transmitted-light observations and for X-ray analysis. The other half was polished and etched on the surface which exposed approximately the center of the sample. Normal metallographic techniques were used for polishing and etching, and a Bausch & Lomb metallograph was used for reflected-light observations. The usual etchant was a 1% HF solution, but to reveal the structural detail in kyanite it was found necessary to etch for about 10 minutes in H_3PO_4 at about 240°C. After identification by the usual optical and X-ray techniques, it was found that the reflected-light observations on polished sections provided the most useful information on what actually was taking place during the run.

None of the techniques as employed here was adequate for the differentiation of sillimanite and mullite. The more careful X-ray approach recently described¹² was not attempted. No significant difference could be seen in the X-ray powder patterns of sillimanite and mullite. This problem is considered in more detail later.

The X-ray diffractometer patterns were obtained with nickel-filtered copper radiation at 2° 2 θ per minute and a chart speed of 0.4 in. per minute. As is often the case with crystals with a good cleavage, special precaution must be taken to avoid preferred orientation during the preparation of a slide of kyanite for an X-ray diffractometer pattern. Pertinent peaks showing intensity variations as a function of preferred orientation are found at 46°, 46.7°, 67.7°, and 69.7° 2 θ (Cu $K\alpha$). A slide with preferred orientation made by the settling of kyanite grains out of a liquid shows high-intensity peaks at 46° and 69.7° 2 θ and low-intensity peaks at 46.7° and 67.7°.

A more random orientation obtained by sprinkling kyanite grains onto a grease smear on a slide, or as found in the usual synthetic kyanite pattern in which grains are small and held in a more random arrangement by other phases, shows complete reversal of these intensities. Similar intensity reversals for natural and synthetic kyanite for the peaks between 45° and 47° 2 θ (Cu $K\alpha$) are seen in the patterns given by Clark *et al.*¹

III. Experimental Results

(1) General

The results of experiments in terms of each of the different starting materials are given in Tables I through IV† and shown graphically in Figs. 3 through 6.

An inspection of the data shows that most of the runs were of short duration (of the order of 2 to 45 minutes) and most of the results probably represent nonequilibrium conditions. The interpretation of what constitutes equilibrium

* The question mark after "sillimanite" throughout this paper indicates that the identification of this phase was doubtful, as discussed later.

¹² S. O. Agrell and J. V. Smith, "Cell Dimensions, Solid Solution, Polymorphism, and Identification of Mullite and Sillimanite," *J. Am. Ceram. Soc.*, **43** [2] 69-76 (1960).

† Tables I through IV have been deposited as Document No. 7865 with the ADI Auxiliary Publications Project, Photoduplication Service, Library of Congress, Washington 25, D. C. A copy may be secured by citing the document number and by remitting \$1.25 for photoprints or \$1.25 for 35-mm microfilm. Advance payment is required. Make checks or money orders payable to: Chief Photoduplication Service, Library of Congress.

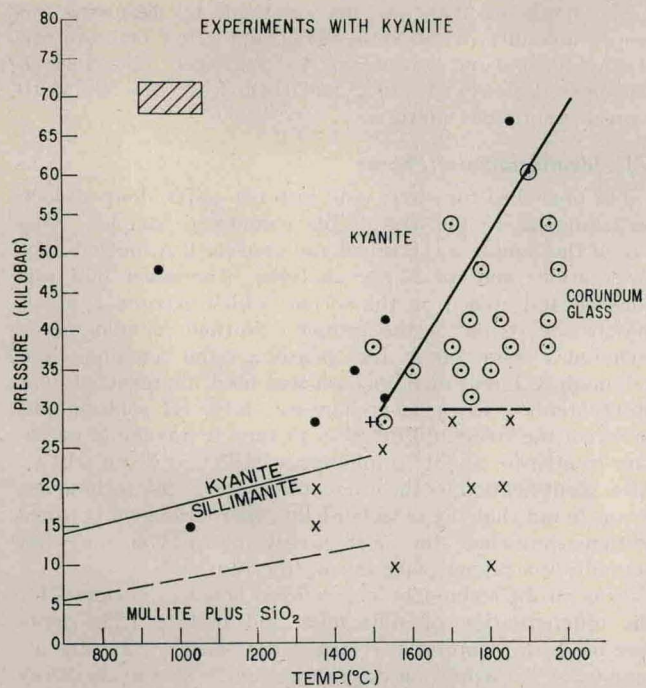


Fig. 3. Kyanite decomposition curve. Data for this figure are given in Table I. Primary-phase regions are labeled in this figure and in Figs. 4, 5, and 6 on the basis of an equilibrium assemblage as interpreted from the data. Symbols indicate actual nonequilibrium assemblages identified in the quenched runs as listed in the tables. Lighter lines are the results from footnotes 1 and 2. Rectangle defines uncertainty of pressure and temperature measurement associated with each point. ● = kyanite; ○ = kyanite, corundum, glass; × = sillimanite (?), corundum, glass; + = sillimanite (?), glass, kyanite.

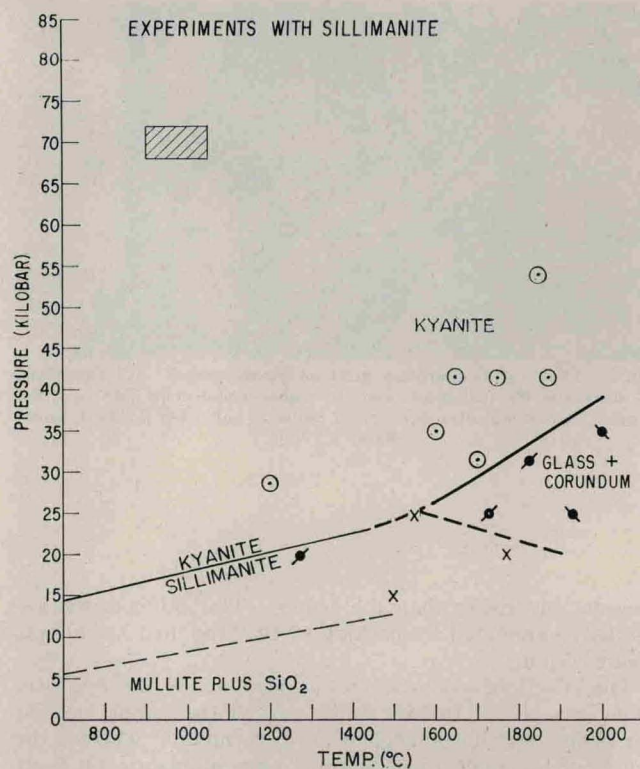


Fig. 5. Formation of kyanite from sillimanite. Data for this figure are given in Table III. ○ = kyanite, corundum, glass; ● = corundum, glass; × = sillimanite (?), corundum, glass; ● = glass, corundum, quartz.

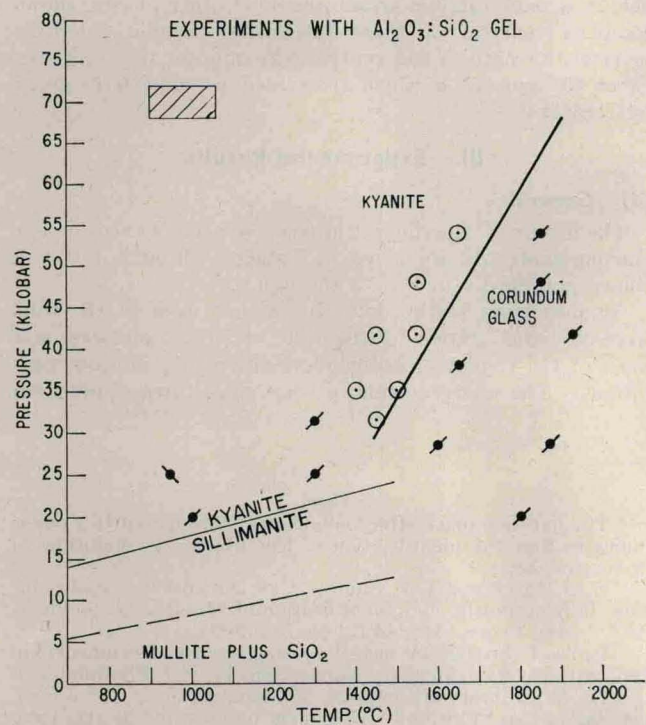


Fig. 4. Formation of kyanite from $Al_2O_3:SiO_2$ gel. Data for this figure are given in Table II. ○ = kyanite, corundum, glass; ● = corundum, glass; ● = corundum, quartz.

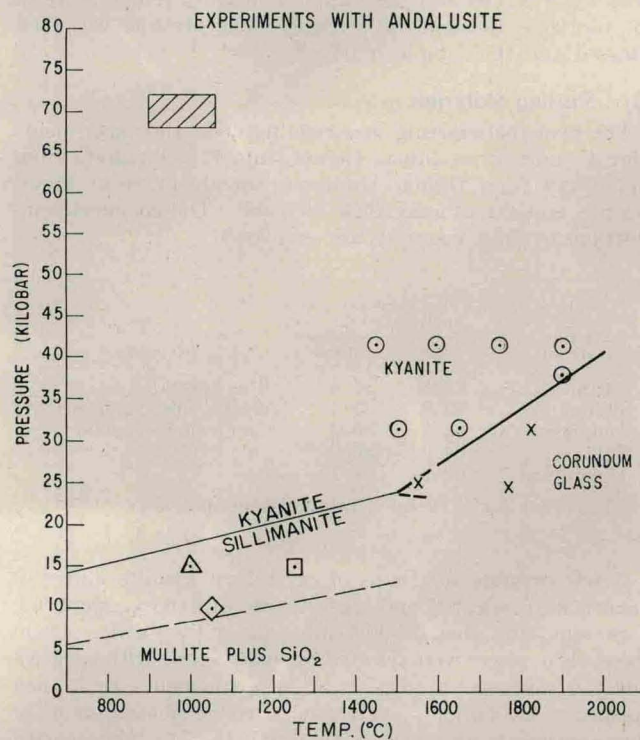


Fig. 6. Formation of kyanite from andalusite. Data for this figure are given in Table IV. ○ = kyanite, corundum, glass; × = sillimanite (?), corundum, glass; ◇ = andalusite; □ = sillimanite (?), corundum, quartz; △ = andalusite, corundum, quartz.